Published in final edited form as:
*Nat Chem Biol*. 2015 December ; 11(12): 952–954. doi:10.1038/nchembio.1933.

# Light-assisted small molecule screening against protein kinases

**Álvaro Inglés-Prieto**[1], **Eva Reichhart**[1], **Markus K. Muellner**[2], **Matthias Nowak**[1], **Sebastian M. Nijman**[2,4], **Michael Grusch**[3], and **Harald Janovjak**[1,*]

[1]Institute of Science and Technology Austria (IST Austria), 3400 Klosterneuburg, Austria

[2]CeMM-Research Center for Molecular Medicine of the Austrian Academy of Sciences, 1090 Vienna, Austria

[3]Institute of Cancer Research, Department of Medicine I, Comprehensive Cancer Center Vienna, Medical University of Vienna, 1090 Vienna, Austria

## Abstract

High-throughput live-cell screens are intricate elements of systems biology studies and drug discovery pipelines. Here, we demonstrate an optogenetics-assisted method that obviates the addition of chemical activators and reporters, reduces the number of operational steps and increases information content in a cell-based small molecule screen against human protein kinases including an orphan receptor tyrosine kinase. This blueprint for all-optical screening can be adapted to many drug targets and cellular processes.

Over the past decades, many chemical processes have been improved by replacing additives, such as catalysts, initiators or emulsifiers, with physical stimuli, such as light or ultrasound[1-4]. Although replacement results in reduced cost, increased robustness and improved sustainability, this general principle has not found many adaptations in chemical biology. Automated screens using living cells are essential in the identification and characterization of small molecules that act on disease-related proteins and cellular pathways. However, in many cell-based screens the need to add reagents that alter or report on cell activity results in complex operational design, high cost and sources of error. Furthermore, mammalian cells are sensitive to environmental perturbations (e.g. temperature or ionic strength) and subject to inherent variability. In neurobiology and cell biology, optogenetics and photopharmacology have recently harnessed the power of light to



*Correspondence and requests for materials should be addressed to H.J. harald@ist.ac.at.
[4]Present address: Ludwig Institute for Cancer Research, NDM Research Building, Roosevelt Drive, Headington, Oxford OX3 7XR, United Kingdom.

**Author contributions**

A.I.P. designed, performed and analyzed all-optical experiments. E.R. designed, performed and analyzed internal reference experiments. M.K.M., M.N., S.M.N. and M.G. designed inhibitor library and experiments and provided reagents. H.J. conceived and supervised the project and designed and analyzed experiments. A.I.P., E.R. and H.J. wrote the paper.

**Competing financial interests statement**

The authors declare no competing financial interests.

**Additional information**

Supplementary information is available in the online version of the paper.


Europe PMC Funders Author Manuscripts

manipulate the behavior of cells and animals non-invasively and with high spatial and temporal precision[5-7]. Here, we developed an optogenetics-assisted, cell-based screening method that interrogates receptor tyrosine kinases (RTKs) and the mitogen-activated protein kinase/extracellular signal-regulated kinase (MAPK/ERK) pathway comprising one G-protein (Ras) and three intracellular kinases (Raf, MEK and ERK). We demonstrate that in this screening method the use of light for activation *and* detection of cell signaling obviated the need for addition of reagents, limited the number of operational steps and provided new strategies to increase specificity and counter variability.

The MAPK/ERK pathway is activated by RTKs and regulates cell survival, proliferation and differentiation. Modulators of the MAPK/ERK pathway, RTKs and other protein kinases are pursued as new therapeutics in cancer and metabolic and neurodegenerative disorders. We first engineered human embryonic kidney 293 (HEK293) cells that contain light-activated RTKs and a genetic fluorescent MAPK/ERK pathway reporter (Fig. 1a). The light-activated RTKs (also called 'Opto-RTKs') are modified growth factor receptors that are insensitive to their natural ligands but activated by blue light-induced homodimerization through incorporation of the light-oxygen-voltage-sensing (LOV) domain of aureochrome1 from *V. frigida*[8] (Supplementary Results, Supplementary Fig. 1). We initially employed two Opto-RTKs, the light-activated murine fibroblast growth factor receptor 1 (Opto-mFGFR1) and the light-activated human epidermal growth factor receptor (Opto-hEGFR). In the fluorescent reporter (SRE-GFP), tandem repeats of serum response element (SRE)[9], an enhancer sequence responsive to signaling pathways including the MAPK/ERK pathway, precede a gene coding for the green fluorescent protein (GFP). The engineered cells respond to light at a wavelength and intensity suited for Opto-RTK activation ($\lambda$~470 nm, intensity~200 $\mu W/cm^2$) with increased production of GFP (Fig. 1b and Supplementary Fig. 2), and combining Opto-RTKs and GFP reporter thus enables a novel 'all-optical' mode of operation where light was used to activate as well as read cellular signaling. Using this mode of operation, we were able to screen small molecules in the 384-well plate format without addition of reagents to induce or detect pathway activation and with few handling steps (Fig. 1c and Supplementary Fig. 3). This assay was robust (Z'-factor $\geq$ 0.7, **Materials and Methods**) and not influenced by ambient light (Supplementary Fig. 4) or bleaching (Supplementary Fig. 5). In addition, all wells in the 384-well plate were activated at the same time and with nearly identical intensity using light emitting diodes (LEDs) (deviation of intensity <0.05% over the plate, day-to-day variability <0.05%). In a set of kinase inhibitors (Supplementary Table 1), three molecules inhibited the mFGFR1-MAPK/ERK-axis by >50%, and these molecules are known kinase inhibitors of FGFR1 or of MAPK/ERK pathway components (Fig. 1c, d and Supplementary Fig. 6). To demonstrate the ability to identify whether ligands act at the receptor or downstream pathway, we conducted the same screen with Opto-hEGFR. Unlike FGFR1, which couples to the MAPK/ERK pathway *via* additional FGFR substrate adaptor proteins, EGFR directly activates it. Three molecules inhibited the EGFR1-MAPK/ERK-axis, and these molecules are known kinase inhibitors of EGFR or pathway components (Fig. 1d). Because inhibitors of FGFR1 were not detected in the screen with EGFR and *vice versa*, the method selectively identified those small molecules that specifically act on receptors or common downstream proteins. Collectively, these results demonstrate a cell-based small molecule screen in the

384-well format assisted by optogenetics. The method functions without added reagents and a reduced number of operational steps as physical contact to the living cells was not required.

Because peptides or other agonists are not required, the all-optical method can also screen against 'orphan' receptors, i.e. receptors for which native ligands are not known. To demonstrate optical control of an orphan receptor, we first identified human orphan RTKs through *de novo* database and bioinformatics analysis (Supplementary Fig. 7). The database search reported human ROS1 (hROS1), a proto-oncogene orphan RTK that is activated by protein fusion in a variety of tumor cell types[10, 11]. To engineer a light-activated variant of human hROS1 (Opto-hROS1), we fused the dimerizing LOV domain to the intracellular domain of hROS1 (Supplementary Fig. 8). When testing the kinase inhibitor library against Opto-hROS1, we found three molecules that inhibited the hROS1-MAPK/ERK-axis (Supplementary Fig. 9). Two of these molecules (crizotinib and GSK-1120212) are known kinase inhibitors of hROS1 and pathway components. The third molecule (AV-951[12]) was active specifically against hROS1 but not mFGFR1 or hEGFR (Supplementary Fig. 10). Notably, AV-951 was previously not assigned to inhibit hROS1.

We next extended the method to increase information content in cell-based screens. First, we demonstrate that a second, spectrally-distinct FP (e.g. mKate2[13]) can be incorporated and detected separately from GFP (Supplementary Fig. 10). If expressed constitutively, this second protein can report small molecules that inhibit gene transcription and protein translation/folding[14], potential assay confounders. As GFP exhibits fluorescence in the same wavelength range as many small molecules in screening collections, a red FP may generally improve assay performance. Second, we tested whether the ability to spatially focus activation can improve the method. Stimulation of optogenetic tools is often realized using custom-built hardware and continuous illumination[15-17]. However, microplate readers commonly part of screening platforms employ discontinuous flash lamps. We thus tested if flashes provide sufficient intensity to activate optogenetic proteins and found that 900 blue light flashes (2 μs duration, 9 W average power of lamp) resulted in robust MAPK/ERK pathway activation in SPC212 cells expressing Opto-mFGFR1 (Fig. 2a to c). Using a light guide-lens assembly, we then confined flash lamp stimulation to the center of single wells (area~3.14 $mm^2$) while leaving the well periphery unstimulated (Fig. 2d, e). We thereby created two cell populations (activated center population and silent peripheral population) within each well, and we exploited these populations to obtain high-content measurements. When testing small molecules, we found that inactive molecules left centers *activated* and peripheries *silent*, inhibitory molecules resulted in *silent* centers and *silent* peripheries, and activators resulted in *activated* centers and *activated* peripheries (Fig. 2f). This result showed that probing two cell populations in a single well was sufficient to test for inhibitory or activating effects of a small molecule. In further experiments, one cell population may also serve as a local control for others. Because trial and control are performed under identical conditions in the same well, the influence of environmental perturbations on measurement outcome may be reduced. These experiments can be directly transferred to high-throughput platform microplate readers without the need for specialized instrumentation.

Europe PMC Funders Author Manuscripts

In summary, we demonstrate that incorporation of optogenetics enabled cell-based small molecule screens without additives but minimal operational steps and increased information content. Light acted as a universal ligand for receptors of different families (e.g. FGFR1, EGFR or ROS1), but, at the same time, was specific to stimulate the genetically-engineered receptors. Interference from endogenous receptors that may be also activated by added ligands can be excluded, which is particularly desirable when targeting receptors for which specific ligands are not available. For instance, in our experiments EGF or FGF2 will have bound to several receptor proteins expressed in these cells (FGFR1, FGFR2, FGFR3, FGFR-like 1 and EGFR), while Opto-RTK activation was specific to the engineered receptor. Activation by light may be in in real-time to reveal new insights into molecular inhibition and cellular signaling mechanisms. For instance, the interaction between small molecules and proteins can be activation-state dependent[18, 19], and the duration and frequency of activation can determine choice of pathway or functional outcome[20, 21]. The ability to switch signals on with temporal precision and tunable strength, even within one well, may explore these phenomena in a systematic and automated manner. This may be of particular use when exploring ‘mutagenesis space’ in genetic libraries and the method is compatible with transient cell transfection. We further foresee the extension and adaptation of this approach to other drug targets to be straightforward because of an increasing number of available optogenetic tools and fluorescent reporters.

## Online Methods

### Kinase inhibitor library

Small molecules are listed in Supplementary Table 1. Out of the tested 68 small molecules, 62 molecules target protein kinases.

### Gene constructs

Opto-mFGFR1 and Opto-hEGFR in pcDNA3.1(-) (Life Technologies) were described previously[8]. Identification of ROS1 and genetic engineering of Opto-hROS1 is described below. The SRE-GFP reporter vector and the vector containing MonsterGFP under the control of the CMV promoter were obtained from Qiagen/SA Biosciences. mKate2 was obtained from D.M. Chudakov (Shemiakin-Ovchinnikov Institute of Bioorganic Chemistry)/ Evrogen[13] and subcloned into pcDNA3.1(-) using polymerase chain reaction.

### Cell culture and transfection

Malignant pleural mesothelioma SPC212 cells were kindly provided by R. Stahel (University of Zurich) and HEK293 were derived by F.L. Graham (McMaster University). Malignant pleural mesothelioma SPC212 cells stably expressing Opto-mFGFR1[8] and HEK293 cells were maintained in RPMI1640 and DMEM, resp., in a humidified incubator with 5% $CO_2$ atmosphere. Media were supplemented with 10% FBS, 100 U/ml penicillin and 0.1 mg/ml streptomycin, and RPMI1640 was additionally supplemented with 2 mM L-Glutamine. For transfection of HEK293 cells, $2\times10^6$ cells were seeded in 60 mm cell culture dishes coated with poly-L-ornithine (PLO, Sigma). Cells were transfected with 4.04 to 8.04 μg total DNA per dish (receptor, pcDNA3.1(-) empty vector, and reporter at a ratio of 1:50:50 or 1:100:100) using polyethylenimine (Polysciences). For mock transfected cells

(Fig. 1b and Supplementary Fig. 2, “HEK293”), receptor vector was omitted in the transfection mixture. For experiments with mKate2[13] (Supplementary Fig. 11), empty vector was substituted by mKate2 in pcDNA3.1(-). For control experiments with MonsterGFP (Supplementary Fig. 5), reporter vector and receptor vector was substituted by vector containing MonsterGFP under the control of the CMV promoter.

### Custom incubator for light stimulation of well plates

A thermoelectric incubator (PT2499, ExoTerra) was equipped with 300 RGB LEDs (5050SMD, $\lambda_{max} \approx 630$ nm (red light), $\lambda_{max} \approx 530$ nm (green light), $\lambda_{max} \approx 470$ nm (blue light), bandwidth $\approx \pm 5$ nm). Light intensity was controlled with a dimmer and measured with a digital power meter (PM120VA, Thorlabs). Blue light intensity at maximal output was 247 μW/cm$^2$. Light of this intensity is sufficient for activation and well tolerated by mammalian cells without signs of toxicity even for extended periods of time. Hardware to maintain a $CO_2$ atmosphere is not required if medium supplemented with HEPES (25 mM) is used during light stimulation (see below). To measure profile of light distribution, the sensor of the power meter was mounted on a holder and moved in 1 cm steps. Intensity was recorded and deviation between highest and lowest intensity was calculated ($\Delta$<0.13 μW/cm$^2$). Day-to-day variability of light was measured in the same way but on several days distributed over one week ($\Delta$<0.13 μW/cm$^2$). For evaluation of the effect of ambient light (Supplementary Fig. 4), cells were stimulated immediately after seeding with white light of comparable intensity to that encountered in a dim room.

### All-optical drug screening against RTKs and the MAPK/ERK pathway

The workflow is depicted in Supplementary Fig. 3. Transfected HEK293 cells were kept in DMEM (supplemented with 5% FBS and no antibiotics; “D5-AB” medium) for 6 h. Afterwards, 5’000 to 20’000 cells were seeded in each well of 384-well plates (3712, Corning) in low-fluorescence medium (FlouroBrite™, Life Technologies, supplemented with 25 mM HEPES, 0.5% FBS, 100 U/ml penicillin and 0.1 mg/ml streptomycin, pH 7.5; “COI” medium). Small molecules were added and after 1 h cells were stimulated with blue light in a custom incubator (see above). Unstimulated cells were kept in the dark by covering selected wells on the same 384-well plate. GFP fluorescence was then measured in a microplate reader (Synergy H1, BioTek) at the optimized excitation wavelength of 500 ± 5 nm and emission wavelength of 535 ± 5 nm (10 measurements per well, measurement duration: 10 ms, gain: 90 to 130). We found that 384-well plates exhibit fluorescence in the blue-green part of the light spectrum (Supplementary Fig. 11), and optimization of the excitation wavelength allowed for improved signal to noise ratio. mKate2 fluorescence was measured at excitation wavelength of 570 ± 5 nm and emission wavelength of 660 ± 5 nm.

### Identification of Orphan RTKs

Orphan RTKs were identified using the bioinformatics procedure described in Supplementary Fig. 7. Protein family search with the PFAM motif “Pkinase_Tyr” (PF07714) at the Wellcome Trust Sanger Institute (http://pfam.xfam.org/)[22] retrieved a comprehensive list of human Tyr kinases. This PFAM motif is a good representative of kinase domains found in RTKs (we confirmed that it is found in members of diverse RTK families, such as fibroblast growth factor receptors, ErbB receptors, Insulin-like growth factor receptor,

neurotrophin receptors, ROR receptors). Retrieval of these sequences was followed by transmembrane helix prediction with TMHMM[23] to retain only sequences with transmembrane helices. To remove sequence redundancy and assign sequence fragments clustering with UCLUST[24] was performed. 69 clusters with a unique candidate sequence each for RTKs were obtained Supplementary Table 2 and orphan RTKs were identified by manual curation.

### Genetic engineering of Opto-ROS1

A sequence coding for the ROS1 gene was obtained from the Mammalian Gene Collection (Dharmacon, GE Life Science). Using inverse PCR, an expression vector was prepared starting from an Opto-mFGFR1 vector in which the mFGFR1 ICD was replaced by two inverted SapI restriction sites. The ROS1 ICD was amplified with oligonucleotides (F: GAT CGC TCT TCA GAC CAT AGA AGA TTA AAG AAT CAA AAA AG, R: GAT CGC TCT TCC AGG ATC AGA CCC ATC TCC ATA TCC ACT G) and PCR and inserted into the vector using ‘Golden Gate’ cloning[25].

### Activation of Opto-RTKs in microplate reader and ERK1/2 phosphorylation

$5\times10^4$ cells per well were seeded in 48-well plates coated with PLO and starved for 24 h in medium containing 0.1% FBS. Small molecules or EGF (5.5 ng/ml) were added to the cells one h prior to onset of light stimulation. A microplate reader equipped with monochromators (Synergy H1, BioTek; 9 W average power of flash lamp, 2 μs flash duration) was repurposed for spatially-confined light stimulation and read-out. For stimulating entire wells, the device’s area scanning mode was configured for a 3×3 matrix with horizontal and vertical point spacing of 2 mm. This protocol was repeated 100 times. For stimulating well centers, the device’s area scanning mode was configured for a 9×9 matrix with minimal point spacing. This protocol was repeated three times. In both protocols, bottom illumination at an excitation wavelength of 470 nm was applied. Cells were then fixed and permeabilised in a solution containing 4% formaldehyde and 1% methanol for 15 min. After washing with PBS three times for 5 min, cells were blocked in 1% BSA, 0.1% Tween in PBS for 30 min and incubated with anti-pERK1/2 (#9101, Cell Signaling Technology, 1:500) for 1 h. After washing with PBS three times for 5 min, signal was developed using the UltraVision LP detection system (Thermo Scientific) and 3,30-diaminobenzidine as chromogen. For read-out, the device’s area scanning mode was configured for a 3×3 with spacing of 3 mm. In some experiments, this protocol was repeated three times with absorbance measurements at 450 nm. Data were normalized to EGF-treated wells and background (SPC212 cells in the dark) was subtracted. Photographs were acquired with a macroscope[26]. This approach can also be used for blue light activation of gene transcription using a different optogenetic system (see below).

### Optimization of excitation wavelength for microplate reader GFP measurements

The microplate reader was used to quantify fluorescence of 384-well plates filled with low-fluorescence media. Emission spectra were acquired at several fixed excitation wavelengths (Supplementary Fig. 12).

### Assay validation and statistical analysis

Z' factors (Supplementary Table 3) were calculated for interleaved-signal format plates following

$$Z'\,\text{factor} = 1 - \frac{3 \times (std\,(c_+) + std\,(c_-))}{|avg\,(c_+) - avg\,(c_-)\,|}$$

where $std\,(c_+)$ and $avg(c_+)$ are the standard deviation and the average of DMSO treated samples, resp., and $std\,(c_-)$ and $avg(c_-)$ are the standard deviation and the average of PD-166866 (INH; final concentration 20μM) treated samples, resp. On each plate, ten columns of DMSO treated samples and ten columns of INH treated samples were tested in groups of two and in alternating order). Z' factors for these plates were ≥0.70 (Supplementary Table 3) and failures were not observed. Percentage of control (POC) values were calculated following:

$$POC = \frac{X_i}{avg\,(c_+)} \times 100$$

where $X_i$ is the measurement of the i$^{th}$ small molecule and $avg(c_+)$ is the average measurement of the DMSO treated samples.

## Supplementary Material

Refer to Web version on PubMed Central for supplementary material.

## Acknowledgements

We thank M. Spanova for technical assistance, R. Chait for photography, X. Amouretti and B. Harris for hardware specifications, R. Stahel (University of Zurich) for mesothelioma cells, and D.M. Chudakov (Shemiakin-Ovchinnikov Institute of Bioorganic Chemistry)/Evrogen (Moscow) for mKate2. This work was supported by grants of the European Union Seventh Framework Programme (CIG-303564 to H.J. and ERC-StG-311166 to S.M.N.), the Human Frontier Science Program (RGY0084_2012 to H.J.), and the Herzfelder Foundation (to M.G.). A.I.P. was supported by a Dan David fellowship and a Ramon Areces fellowship, and E.R. by the graduate program MolecularDrugTargets (Austrian Science Fund) and a FemTech (Austrian Research Promotion Agency) fellowship.

## References for main text

1. Cravotto G, Cintas P. Chem. Soc. Rev. 2006; 35:180–196. [PubMed: 16444299]
2. Bradley M, Grieser F. J. Colloid. Interface Sci. 2002; 251:78–84. [PubMed: 16290704]
3. Asahi R, Morikawa T, Ohwaki T, Aoki K, Taga Y. Science. 2001; 293:269–271. [PubMed: 11452117]
4. Xuan J, Xiao WJ. Angew. Chem. Int. Ed. Engl. 2012; 51:6828–6838. [PubMed: 22711502]
5. Tischer D, Weiner OD. Nat. Rev. Mol. Cell. Biol. 2014; 15:551–558. [PubMed: 25027655]
6. Szobota S, Isacoff EY. Annu. Rev. Biophys. 2010; 39:329–348. [PubMed: 20192766]
7. Fenno L, Yizhar O, Deisseroth K. Annu. Rev. Neurosci. 2011; 34:389–412. [PubMed: 21692661]
8. Grusch M, et al. EMBO J. 2014; 33:1713–1726. [PubMed: 24986882]
9. Mohun T, Garrett N, Treisman R. EMBO J. 1987; 6:667–673. [PubMed: 3582369]
10. Shaw AT, Hsu PP, Awad MM, Engelman JA. Nat Rev Cancer. 2013; 13:772–787. [PubMed: 24132104]

11. Takeuchi K, et al. Nature medicine. 2012; 18:378–381.
12. Jamil MO, Hathaway A, Mehta A. Curr Oncol Rep. 2015; 17:24. [PubMed: 25895472]
13. Shcherbo D, et al. Biochem J. 2009; 418:567–574. [PubMed: 19143658]
14. Crouch SP, Kozlowski R, Slater KJ, Fletcher J. J. Immunol. Methods. 1993; 160:81–88. [PubMed: 7680699]
15. Chen X, Wang X, Du Z, Ma Z, Yang Y. Curr Protoc Chem Biol. 2013; 5:111–129. [PubMed: 23839993]
16. Olson EJ, Hartsough LA, Landry BP, Shroff R, Tabor JJ. Nat Methods. 2014; 11:449–455. [PubMed: 24608181]
17. Richter F, et al. Photochem Photobiol Sci. 2014
18. DiNitto JP, et al. J. Biochem. 2010; 147:601–609. [PubMed: 20147452]
19. Simard JR, et al. J. Am. Chem. Soc. 2009; 131:18478–18488. [PubMed: 19950957]
20. Burke P, Schooler K, Wiley HS. Mol. Biol. Cell. 2001; 12:1897–1910. [PubMed: 11408594]
21. Toettcher JE, Weiner OD, Lim WA. Cell. 2013; 155:1422–1434. [PubMed: 24315106]

## Methods-only References

22. Finn RD, et al. Nucleic Acids Res. 2010; 38:D211–222. [PubMed: 19920124]
23. Krogh A, Larsson B, von Heijne G, Sonnhammer EL. J. Mol. Biol. 2001; 305:567–580. [PubMed: 11152613]
24. Edgar RC. Bioinformatics. 2010; 26:2460–2461. [PubMed: 20709691]
25. Engler C, Marillonnet S. Methods Mol Biol. 2014; 1116:119–131. [PubMed: 24395361]
26. Chait R, Shrestha S, Shah AK, Michel JB, Kishony R. PLoS One. 2010; 5:e15179. [PubMed: 21209699]



Europe PMC Funders Author Manuscripts

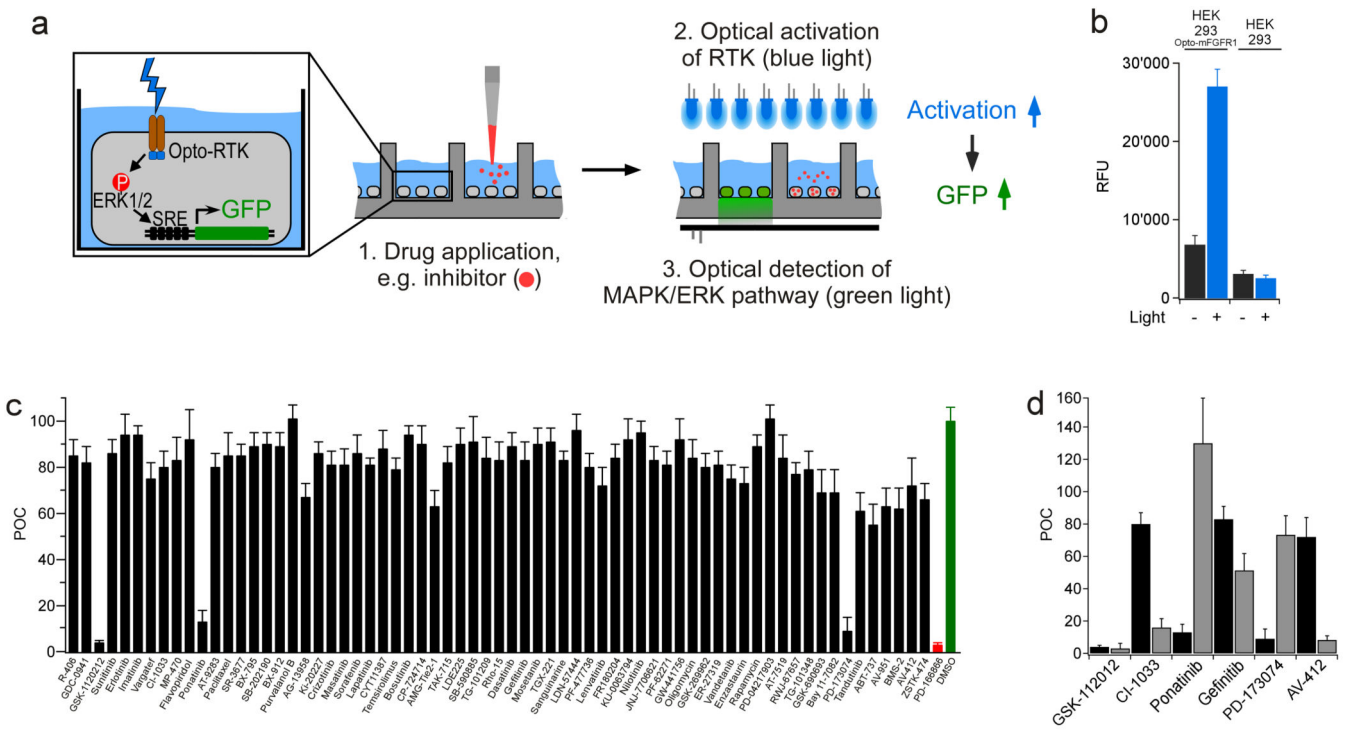


**Figure 1. All-optical screen against RTKs and the MAPK/ERK pathway**

(**a**) HEK293 cells were engineered to contain an Opto-RTK (Opto-mFGFR1, Opto-hEGFR or Opto-hROS1, Supplementary Fig. 1 and Supplementary Fig. 8) and a MAPK/ERK pathway-responsive GFP reporter (SRE-GFP). In all-optical screening, effects of small molecules (e.g. receptor inhibitors or pathway inhibitors) are tested in 384-well plates by first activating the RTK with blue light (λ~470 nm, I~200 μW/cm$^2$) followed by detection of pathway activity using the GFP reporter. In cells treated with inhibitors of RTKs or of components of the MAPK/ERK pathway, GFP expression will be absent. Except for small molecule addition, the process does not require contact to the cells, solution exchange or added reagents (Supplementary Fig. 3). (**b**) Control experiments demonstrating activation of MAPK/ERK pathway by Opto-mFGFR1 and blue light as measured using the GFP reporter. Mean raw fluorescent units (RFU) ± SD (n=3, one representative experiment) are shown. (**c**) All-optical screen against mFGFR1 and MAPK/ERK pathway (68 small molecules, final concentration 5 nM). PD-166866 (final concentration 5 μM), a specific FGFR1 inhibitor, and DMSO were used as controls (red and green bars). Mean percent of control (POC) values ± SEM (n=4, two independent experiments) are shown. (**d**) Comparison of all-optical experiments with Opto-mFGFR1 (black bars) and Opto-hEGFR (grey bars) allow identifying small molecules that specifically inhibit mFGFR1 (ponatinib, PD-173074), hEGFR (CI-1033, AV-412, gefitinib) or downstream proteins of the MAPK/ERK pathway (GSK-1120212). Mean POC values ± SEM (n=4, two independent experiments) are shown.




Europe PMC Funders Author Manuscripts

Europe PMC Funders Author Manuscripts

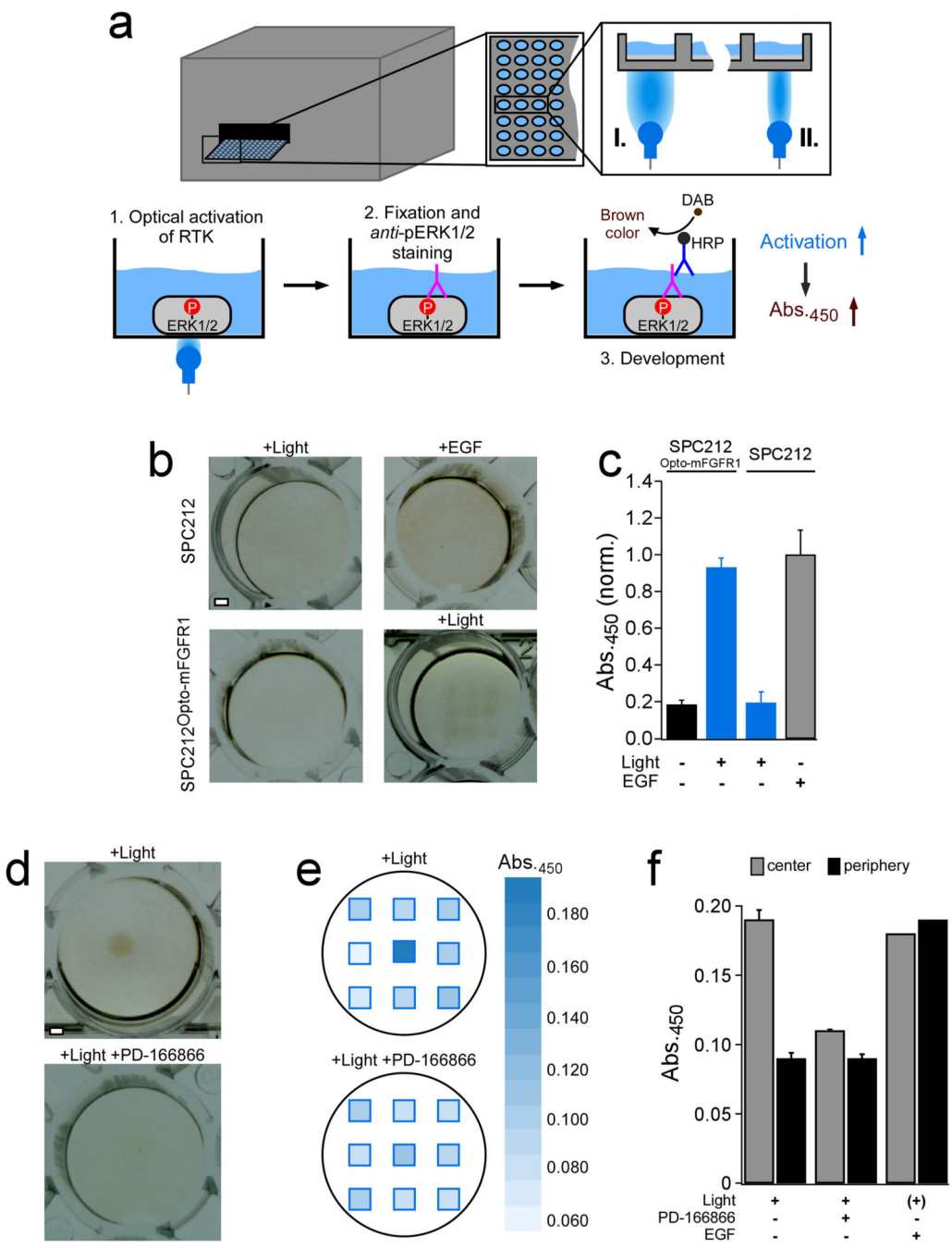


**Figure 2. Optogenetics-enabled, internally-referenced measurement of MAPK/ERK pathway**

(**a**) Whole well (I.) or spatially-confined (II.) light stimulation (λ=470 ± 5 nm) of SPC212$^{Opto\text{-}mFGFR1}$ cells was performed in a microplate reader. 48-well plates were chosen for these experiments to enable visual evaluation after *anti*-pERK1/2 immunohistochemistry (see b and d). (**b**) Raw data photographs of cells stimulated with EGF (5.5 ng/ml) or light (distributed over the well in a 3×3 matrix). MAPK/ERK pathway was activated by EGF in SPC212 cells or light in SPC212$^{Opto\text{-}mFGFR1}$ cells but not in controls. (**c**) Quantification of b. Mean (normalized) absorption values ± SEM (n=9, one representative experiment) are

shown. (**d**) Raw data photographs of local activation (area~3.14 $mm^2$) of the MAPK/ERK pathway by spatially-confined illumination of $SPC212^{Opto\text{-}mFGFR1}$ cells. Activation is limited to the center of the well and inhibited by PD-166866 (final concentration 5 μM). (**e**) Quantification of d. (**f**) Characterization of an inactive molecule (vehicle, left bars), inhibitor (PD-166866, middle bars) or activator (EGF, right bars) through internal references in a single measurement. Mean (normalized) absorption values ± SEM (n=6, 3 and 2 from left to right, two independent experiments) are shown. Scale bar in b and c is 1 mm.



Europe PMC Funders Author Manuscripts